The Momentum Distribution of Normal and Superfluid Liquid ^{4}He

D. M. Ceperley and E. L. Pollock
Lawrence Livermore National Laboratory

ABSTRACT

Path integral methods can be employed to calculate properties of boson systems at any temperature. We have performed a number of simulations of liquid helium and have calculated the momentum distribution as a function of temperature. We find that liquid helium has a condensate below 2K but not above. The momentum distribution is found to be non-Gaussian even in normal liquid helium. We have also calculated the difference in the momentum distribution between a boson system and a distinguishable particle system.

Classical systems always have a simple Maxwellian momentum distribution regardless of temperature and density but quantum systems can in principle have a non-Gaussian momentum distribution. In fact the theory of liquid helium is based on the assumption that for the superfluid there is macroscopic occupation of the zero momentum state. However experimentally verifying this basic property has proved to be difficult. Computer simulation can compute details of the momentum distribution from first principles. Here we will briefly discuss the simulation method and the results that have been obtained to date on helium. Simulation also enables one to do some thought experiments. As an example we will show the effects in helium of removing Bose statistics.

The basic formula needed in quantum Monte carlo method at non-zero temperature was written down by Feynman and Kacs in 1950[1] who related the density matrix of a quantum system to a path integral. One can say equivalantly that a quantum system can be mapped onto a classical system of higher dimension. Before we describe the path integral method let us first specify our model of liquid helium. Helium atoms are assumed to be bosons and described by the non-relativistic Schrödinger equation with the Born-Oppenheimer potential energy function. In calculations done to date we have assumed the atoms interact only in pairs and have used the Aziz[2] (HFDHE2) pair potential. This potential is thought to be accurate on the average to 0.15K/atom out of a total potential energy of -22 K/atom, i.e. better than 1%. Calculations at zero temperature show that the momentum distribution is not very sensitive to the pair interaction.[3-4] Recent experimental measurements and theoretical calculations indicate that this potential needs some slight revision.[5] In order to perform simulations we must work with a

small number of atoms, on the order of 100, and periodic boundary conditions are used to remove most boundary effects. Of course this restriction will limit our ability to perform precise calculations around a phase transition particularly around the lambda region since a second order transition is greatly influenced by the boundaries.

All thermodynamic properties can be obtained as integrals over the many-body density matrix written in configuration space as $\langle R|\exp(-\beta H)|R'\rangle$ where R and R' represent the 3N coordinates of the atoms, H is the Hamiltonian and $\beta=1/kT$. We have the following properties of this density matrix:

1) The density matrix is non-negative for all values of its arguments (R, R' and β) for distinguishable particles. Thus it can be interpreted as a probability distribution and sampled.
2) The convolution of two density matrices yields a density matrix at a lower temperature.

$$\langle R|\exp(-(\beta_1+\beta_2)H)|R'\rangle = \int dR''\langle R|\exp(-\beta_1 H)|R''\rangle\langle R''|\exp(-\beta_2 H)|R'\rangle \quad (1)$$

The integral over R" above is performed with Monte Carlo. The path integral method consists of writing down an explicit analytic expression for the density matrix at high temperature (40 K was used in our calculations) and convoluting on the order of 20 of them together to get down to 2K. The intermediate points (like R" in Eq. (1)) make up the path.

3) At a sufficiently high temperature, the density matrix factorizes into one and two body density matrices.

$$\langle R|\exp(-\tau H)|R'\rangle = \exp[-(R-R')^2/(2\Lambda\tau) - \sum_{i<j} u(r_{ij},r'_{ij};\tau)] + O(\tau^3) \qquad (2)$$

where $\Lambda = \hbar^2/m$. The next order terms in this expansion involve triplets of particles and can be neglected above 40K, as shown by convergence studies with helium.

4) The boson density matrix is obtained from the distinguishable particle density matrix by using the permutation operator to project out the symmetric part.

$$\langle R|\exp(-\beta H)|R'\rangle_B = \sum_P \langle PR|\exp(-\beta H)|R'\rangle/N! \qquad (3)$$

Clearly the Bose density matrix is non-negative, so all thermodynamic properties of helium 4 can be rigorously computed with probabilistic methods. The above equation is interpreted as saying that because the atoms are indistinguishable the labelling of atoms at the end of a path, at R', can be different from that at the beginning, at R. Now because thermodynamic properties are determined by the diagonal part of the density matrix the paths must close on themselves. The density matrix from R to R' is obtained by averaging over all paths which begin at R and end at R'. But the above equation says that path can end at R' or any point PR' where P is a permutation of atoms. It is this additional freedom which gives rise to superfluidity and Bose condensation. At the lambda temperature and below, permutations involve a macroscopic number of atoms. The sum over permutations is also performed with Monte Carlo. Thus the complete specification of the state of the simulation consists

of the coordinates of all of the atoms at all of the intermediate points and the permutation which tells how the path closes on itself.

The above properties of the density matrix are the essential properties. Since the path is described by a probability density, it is much like the Boltzmann distribution for a collection of N ring polymers. Hence we can use simulation methods from classical statistical mechanics to compute averages over the density matrix. Our algorithm uses a generalization of the Metropolis Monte Carlo method. Care must be taken since a naive method would converge extremely slowly since moves of the atomic coordinates must be coupled with moves in permutation space. Our algorithm will be described in detail elsewhere.[6-7]

Since the wave functions in momentum space are the Fourier transforms of the wave functions in coordinate space the density matrix in momentum space is just the transform of the density matrix in coordinate space. The momentum distribution is given by the diagonal element of the momentum space density matrix and in particular the one particle momentum distribution is obtained by integrating over the momenta of all but one particle. Defining the single particle density matrix by:

$$n(\underset{\sim}{r}) = \int d\underset{\sim}{r}_1 d\underset{\sim}{r}_2 \cdots d\underset{\sim}{r}_N \, \langle \underset{\sim}{r}_1, \underset{\sim}{r}_2, \cdots \underset{\sim}{r}_N | \exp(-\beta H) | \underset{\sim}{r}_1 + \underset{\sim}{r}, \underset{\sim}{r}_2, \cdots \underset{\sim}{r}_N \rangle / Z \qquad (5)$$

where Z is the partition function, the probability that an atom has momentum k is the Fourier transform of this single particle density matrix.

$$n_{\underset{\sim}{k}} = (2\pi)^{-3} \int d\underset{\sim}{r} \exp(-i\underset{\sim}{k} \cdot \underset{\sim}{r}) \, n(\underset{\sim}{r}) \qquad (6)$$

Note that in contrast with the thermodynamic properties, calculating the momentum distribution requires the off-diagonal part of the density matrix. It follows that the momentum distribution is normalized as:

$$\int d^3\underset{\sim}{k}\; n_{\underset{\sim}{k}} = 1 \tag{7}$$

and furthermore the kinetic energy is the second moment of the momentum distribution:

$$K = \frac{\Lambda}{2} \int d^3\underset{\sim}{k}\; k^2\; n_{\underset{\sim}{k}} = -\frac{\Lambda}{2}\nabla^2\; n(\underset{\sim}{r})\Big|_{r=0} \tag{8}$$

One obtains the classical Maxwellian distribution by assuming that the magnitude of $\underset{\sim}{r}$ in Eq. (4) is much less than the interparticle spacing and using the high temperature form of Eq. (2) for the density matrix:

$$n_{cl}(r) = \exp[-r^2/(2\Lambda\beta)] \tag{9}$$

To a first approximation quantum effects for distinguishable particles enter by changing the width of the single particle density matrix to reflect the actual kinetic energy instead of 3kT/2

$$n_G(\underset{\sim}{r}) = \exp[-r^2K/(3\Lambda)]$$

Note that the kinetic energy of liquid helium is always greater than 3kT/2 because of the confining effects of the hard cores and reaches a value of 14 K at zero temperature. Thus quantum effects in the momentum distribution are already dominant at 10 K, well above the lambda transition.

For bosons the symmetrization introduces a totally new feature. In calculating the off-diagonal density matrix, the order of the arguments of the density matrix in Eq. (4) is not relevant. That is atom 1 can end up at atom 2's starting place, atom 2 can end up at 3's starting place and finally atom N is free to end up far away from atom 1's starting place. One finds that below the lambda temperature, $n(\underset{\sim}{r})$ does not go to zero at large $\underset{\sim}{r}$ but instead to a constant, n_o. Then its Fourier transform, the momentum distribution will have a delta function at $\underset{\sim}{k}=0$ and n_o will be the fraction of atoms with exactly zero momentum, the condensate. It is the macroscopic permutations which establish both the order parameter of the superfluid state, the phase of the wave function and the condensate.

In order to calculate $n(\underset{\sim}{r})$ we have used two complementary algorithms. The first consists of doing the simulation on the diagonal, and then displacing one atom off the diagonal by a distance $\underset{\sim}{r}$. The permutation and the coordinates of the other intermediate atoms (i.e. the rest of the path) is held fixed. This method is very accurate for computing $n(\underset{\sim}{r})$ at small $\underset{\sim}{r}$, less than 2.5 A, because it can be done simultaneously with computing diagonal properties and because all atoms at all points along the path can be displaced. However beyond 2.5 A the statistical error with this method grows rapidly because the permutation and the rest of the path must be allowed to relax as $\underset{\sim}{r}$ is increased. In the second method one atom is allowed to be off the diagonal. An additional variable, $\underset{\sim}{r}$, the distance between the two ends of the path of that atom, is introduced into the Monte Carlo integration and at each step of the simulation that distance is calculated and recorded. The single particle density matrix is proportional to this end-to-end distribution and the condensate is the value of the distribution function at large $\underset{\sim}{r}$

divided by the value at the origin. An artificial potential between the two ends equal to log $(n_a(r)\ r^2)$ is also applied, so that the simulation will spend roughly the same time at large and small r. Here $n_a(r)$ is an approximate single particle density matrix. The effect of this potential is divided out of the distribution function. This importance sampling improves the statistical resolution of the algorithm. The disadvantage of this second method is that to obtain $n(\underset{\sim}{r})$ one must divide by the value at $\underset{\sim}{r}=0$ and this introduces a large uncertainty because of the long correlation time of the end-to-end distribution function. The results we present here are obtained by using the results of the first method for r<2.5 Å smoothly matched onto the distribution function results obtained by the second method for r>2.5 Å.

Calculation of the single particle density matrix is more difficult with path integrals than with the zero-temperature Green's Function Monte Carlo method. At zero temperature the density matrix factors into a product of two ground state wave functions and so it is not necessary to find a path connecting $\underset{\sim}{r}_1$ with $\underset{\sim}{r}_1+\underset{\sim}{r}$ but only to evaluate the wavefunction at those two points. However this complication of the path integral method is more than repaid by the ability to calculate the momentum distribution at all temperatures and for both distinguishable particles and bosons. With path integrals one can see the change in the momentum distribution as the system is cooled through the lambda transition.

In this paper we will only give results of our calculations for the momentum distribution since other thermodynamic properties have been already published.[7] In general agreement with experiment is good for these other properties. Discrepancies near the lambda temperature result from the small number of atoms in the simulations since most runs were done with 64 atoms.

The momentum distribution for temperatures ranging from 1.18 K to 3.33 K along SVP are given in Table I. We believe that these momentum distributions are in reasonable agreement with the analysis of neutron inelastic scattering measurements[8-10] at high momentum transfers. Also included in Table I is the momentum distribution of distinguishable helium atoms at 2.22 °K. To obtain distinguishable statistics one simply requires that the permutation remain as the identity permutation during the simulation.

The structure factor, S(k) is shown in Fig. 1 at 2.0 K and compared with the neutron scattering measurements[11] at 1.97 K. The differences are less than 0.02 everywhere. This implies that our model of helium is describing the structure of the liquid well, even in the vicinity of the superfluid transition. The inadequacies of the pair potential and the high temperature density matrix will affect S(k) and n_k in a similar fashion.

In Fig. 2 is shown the off-diagonal density matrix at several temperatures. The right hand side of this figure shows an enlargement of its long-range behavior. At 3.33 K, n(r) is clearly going to zero at large r. However at 2.22 K, n(r) still has a value of 0.02 at the edge of the simulation box. Since this temperature is above the experimental lambda temperature of 2.17 K, theory will predict that the asymptotic value of n(r) should be zero. Simulations of much larger systems are needed to demonstrate this. At 1.18 K, the value of the density matrix at the edge of the box has reached 0.07 which is consistent within the statistical errors with the zero temperature result[4] of 0.09. Figure 3 shows the condensate fraction, as obtained by averaging n(r) between 5.5 A and 7.0 A., as a function of temperature. They are constant below 2 K and rapidly fall to zero above 2 K. These values are consistent with experimental measurements.[8-10]

Figure 4 shows the momentum distribution of the non-condensed atoms. This is computed by fourier transforming $n(r)-n_o$. Above 2.5/A there is considerable statistical error coming from the effects of fourier transforming noisy data. The temperature dependance of n_k is confined to the region $k < 1/A$. One can see from Table I that the distribution at low momentum has a maximum variation of about 20%. The largest change comes from turning off the Bose statistics. The difference between the momentum distribution with and without Bose statistics at 2.22 K is shown in Fig. 5. As Bose statistics are turned on, we find that the region of momentum less than 1.4/A is depleted. Half of those atoms go to form the condensate and the other half get excited to momenta between 1.4 /A and 2.5/A. The net result is that the kinetic energy is approximately the same in the two liquids.

Figures 6 and 7 show the deviation of the momentum distribution from a Gaussian form. In Fig. 6 is plotted the logarithm of the single particle density matrix versus the squared distance scaled by the kinetic energy. The straight line represents a Gaussian distribution. The single particle density matrix decays more slowly than a Gaussian distribution at all temperatures, both above and below the lambda transition and independant of whether the atoms are bosons or not. Figure 7 shows the non-Gaussian character of the momentum distribution with the dashed line representing a Gaussian distribution with the correct kinetic energy. It is seen that there is an enhancement of atoms with momenta less than 1.4/A for all the temperatures studied. At both finite temperature and zero temperature there appears a shoulder in the distribution function at about 2.5/A. This has also been observed experimentally.[10,12] This shoulder is not present for distinguishable particles.

It has been suggested[13] that one can determine the superfluid density, n_s, of liquid helium by observing the large r behavior of n(r) since:

$$n(r)/n_o = \begin{cases} \dfrac{1}{4\pi\Lambda n_s \beta r} & \beta\hbar c < r \\ \dfrac{\hbar c}{4\pi^2 \Lambda n_s r^2} & \beta\hbar c > r \end{cases}$$

where c is the sound speed (at low temperatures and pressures SVP $\hbar c = 18^{\circ}K$ Å). Our present simulations are performed with systems which are too small to observe this exact asymptotic behavior but it may be possible to verify these relationships for systems with several thousand atoms. In the meantime we have calculated the superfluid fraction directly using the momentum–momentum correlation function. The calculations are in rough agreement with experiment and will be described elsewhere.[14]

Monte Carlo simulations have allowed the first look at the momentum distributions of strongly interacting quantum systems. We anticipate that as these methods become more accurate a microscopic understanding and characterization of the lambda transition in helium and of the superfluid state will result.

REFERENCES

1. R. P. Feynman, "Statistical Mechanics," Benjamin, New York, 1972; M. Kac, "Probability and Related Topics in Physical Science," Interscience, New York, 1959.
2. R. A. Aziz, V. P. S. Nain, J. S. Carley, W. L. Taylor and G. T. McConville, J. Chem. Phys. 70, 4330 (1979).
3. P. A. Whitlock, D. M. Ceperley, G. V. Chester and M. H. Kalos, Phys. Rev. B19, 5598 (1979).
4. M. H. Kalos, M. A. Lee, P. A. Whitlock and G. V. Chester, Phys. Rev. B24, 115 (1981).
5. R. A. Aziz, this volume and D. M. Ceperley and H. Partridge, J. Chem. Phys. 84, 820 (1986).
6. E. L. Pollock and D. M. Ceperley, Phys. Rev. B30, 2555 (1984).
7. D. M. Ceperley and E. L. Pollock, Phys. Rev. Lett. 56, 351 (1986).
8. P. E. Sokol, R. O. Simmons, D. L. Price and R. O. Hilleke, preprint, 1986.
9. H. A. Mook, Phys. Rev. Lett. 51, 1454 (1983).
10. V. F. Sears, E. L. Svensson, P. Martel and A. D. B. Woods, Phys. Rev. Lett. 49, 279 (1982).
11. V. F. Sears, F. C. Svensson, A. D. B. Woods, and P. Martel, Atomic Energy of Canada, Report 6779 (1979).
12. A. D. B. Woods and V. F. Sears, Phys. Rev. Lett. 39, 415 (1977).
13. A. Griffin, Phys. Rev. B30, 5057 (1984).
14. E. L. Pollock, to be published.
15. P. Whitlock, private communication.

FIGURE CAPTIONS

Fig.1 The structure factor at 2 K as computed by path integral Monte Carlo (solid line) and at 1.97 K as measured (Ref. 4) by neutron scattering (solid circles). Both are at SVP.

Fig. 2 The single particle density matrix at 1.18 K (top curve and open circles) 2.22K (middle curve and closed circles) and 3.33 K (lower curve and open squares). Beyond 3 Å the vertical axis is enlarged 10 times and the interpolating curves are omitted. The crosses denote the ground state results (Ref. 4) which are indistinguishable from the 1.18 K results for $r < 3$ Å on this graph.

Fig. 3 The percentage of atoms with zero momentum $n_o(T)$ at SVP. The indicated value at T=0 is from Ref. 4.

Fig. 4 The momentum distribution at 3.33 K (solid curve), 2.22 K (dashed curve) 1.18 K (open circles) and for distinguishable particles at 2.22 K (solid circles).

Fig. 5 The difference between the distinguishable particle momentum distribution and the boson momentum distribution at 2.22 K versus the momentum. The region 0 to 1.4/Å is depleted of distinguishable atoms. Half go into the condensate and half go into higher momentum states, between 1.4/Å and 2.5/Å, so that the total kinetic energy is roughly unaltered by the change in statistics.

Fig. 6 The logarithm of the single particle density matrix versus the square of the distance for the indicated temperatures. The staight line represents the expected behavior if the momentum distribution of the non-condensed particles were Gaussian. By construction all curves have a slope of 1 at the origin. The actual n(r)'s decay more slowly than a Gaussian.

Fig. 7 The logarithm of the momentum distribution versus the square of the momentum. The dashed line represents a Gaussian momentum distribution with the same kinetic energy. The solid line is for distinguishable atoms at 2.22 K, the crosses for bosons at 2.22 K and the open circles the ground state momentum distribution.[15]

Table I. The momentum distribution of liquid helim as computed by path integral Monte Carlo. n_o is the condensate faction, n_k is the distribution of non-condensed atoms. The column marked (*) is for distinguishable atoms, the others are bosons.

T(°K)		1.18	1.54	1.82	2.22	2.22*	2.50	3.33
$\rho(\text{Å}^{-3})$		0.02182	0.02183	0.02186	0.02197	0.02197	0.02179	0.02072
n_o		0.069 ±0.010	0.087 ±0.010	0.063 ±0.010	0.027 ±0.005	0	0.013 ±0.003	0.003 ±0.001
Kinetic Energy (°K)		14.2	14.4	14.7	15.9	16.0	15.9	16.0
	$k(\text{Å}^{-1})$							
	0.02	0.1013	0.0884	0.0947	0.1034	0.1295	0.1162	0.1120
	0.27	0.0966	0.0861	0.0907	0.0975	0.1202	0.1080	0.1041
n_k	0.52	0.0849	0.0785	0.0800	0.0829	0.0988	0.0894	0.0860
(Å^3)	0.77	0.0683	0.0647	0.0643	0.0636	0.0725	0.0667	0.0643
	1.02	0.0492	0.0471	0.0467	0.0446	0.0484	0.0459	0.0446
	1.27	0.0308	0.0299	0.0305	0.0294	0.0302	0.0295	0.0294
	1.52	0.0163	0.0158	0.0174	0.0182	0.0178	0.0175	0.0183
	1.77	0.0073	0.0066	0.0084	0.0102	0.0099	0.0094	0.0104
	2.02	0.0034	0.0032	0.0040	0.0053	0.0051	0.0049	0.0057
	2.27	0.0023	0.0032	0.0027	0.0030	0.0024	0.0030	0.0034
	2.52	0.0018	0.0029	0.0022	0.0019	0.0011	0.0021	0.0021
	2.77	0.0013	0.0015	0.0014	0.0011	0.0006	0.0014	0.0013
	3.02	0.0009	0.0005	0.0007	0.0004	0.0004	0.0008	0.0007
	3.27	0.0008	0.0005	0.0004	0.0003	0.0003	0.0005	0.0005
	3.52	0.0005	0.0004	0.0000	0.0002	0.0003	0.0003	0.0002

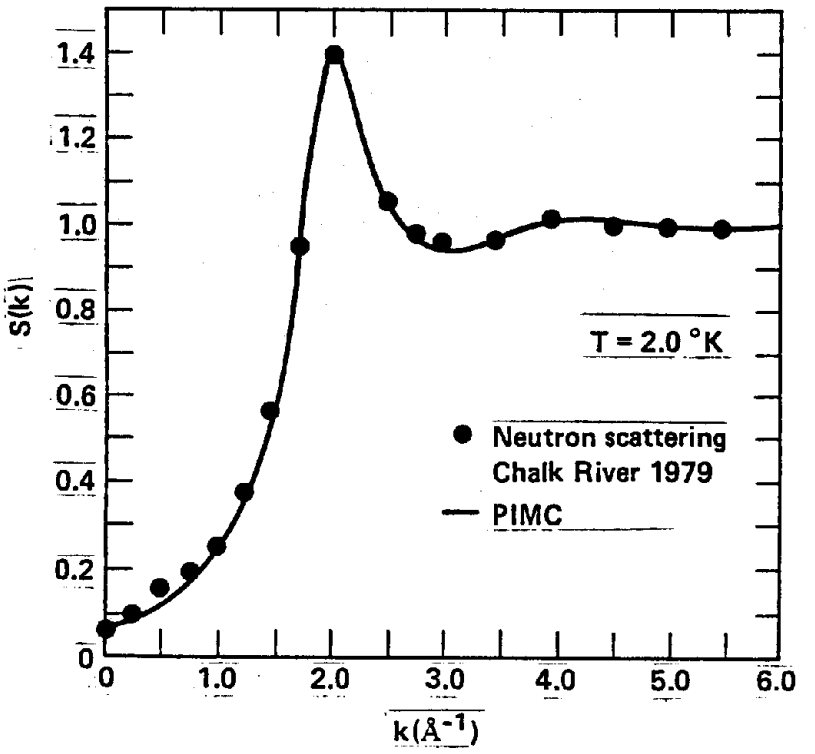
S(k)
1.4
1.2
1.0
0.8
0.6
0.4
0.2
0
0
1.0
2.0
3.0
4.0
5.0
6.0
k(Å⁻¹)
T = 2.0 °K
Neutron scattering
Chalk River 1979
PIMC

Figure 1

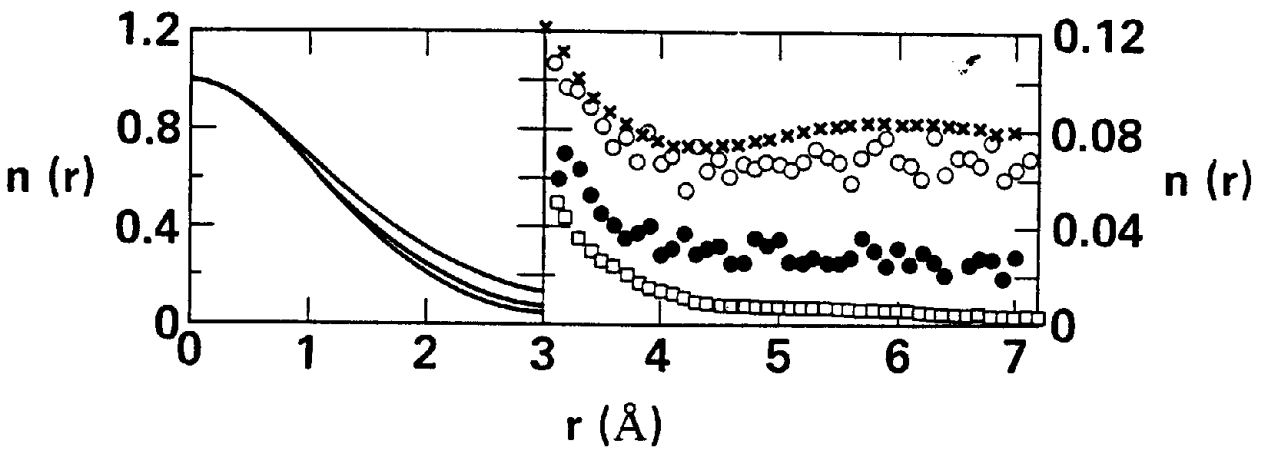

Figure 2

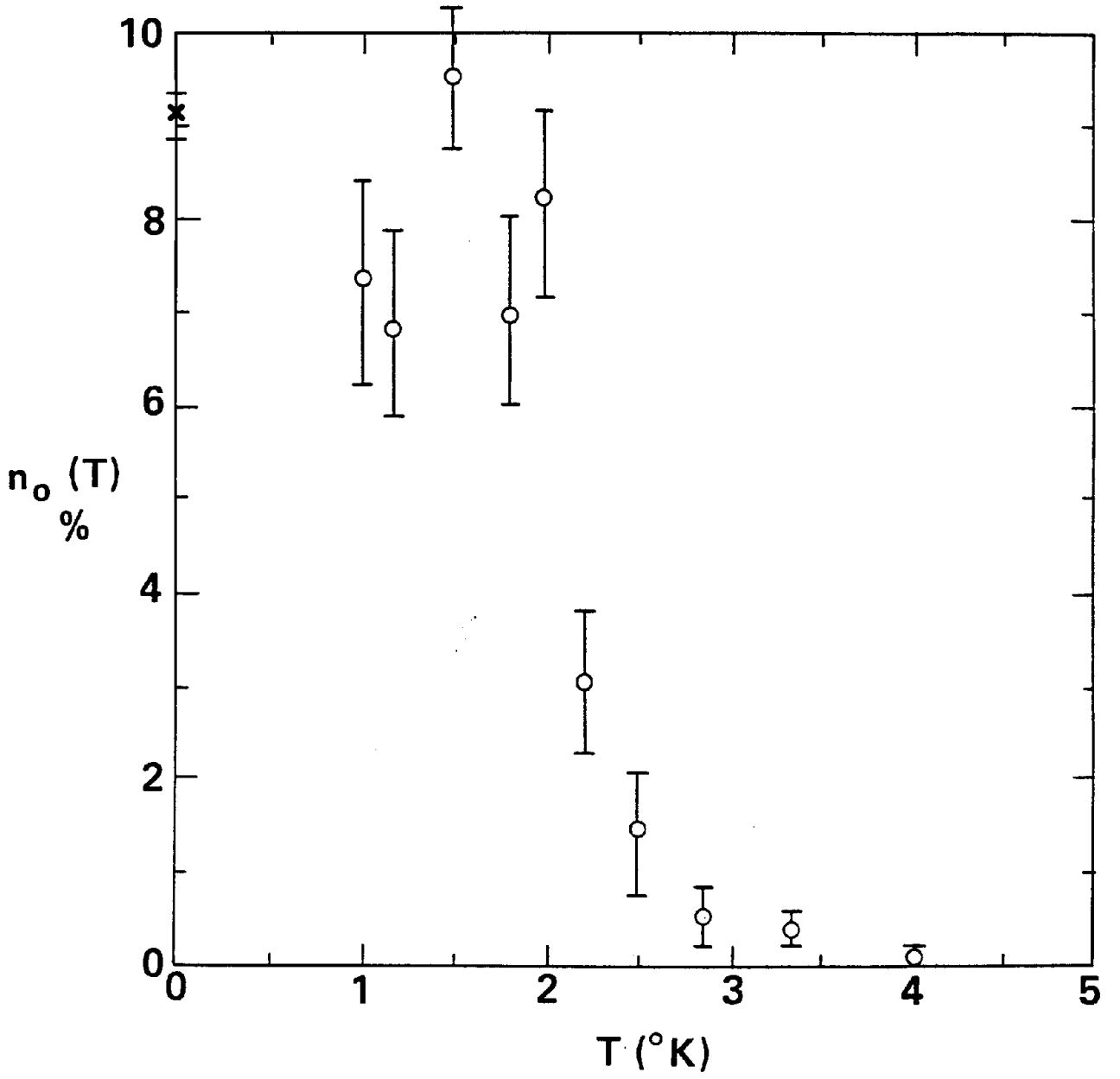

Figure 3

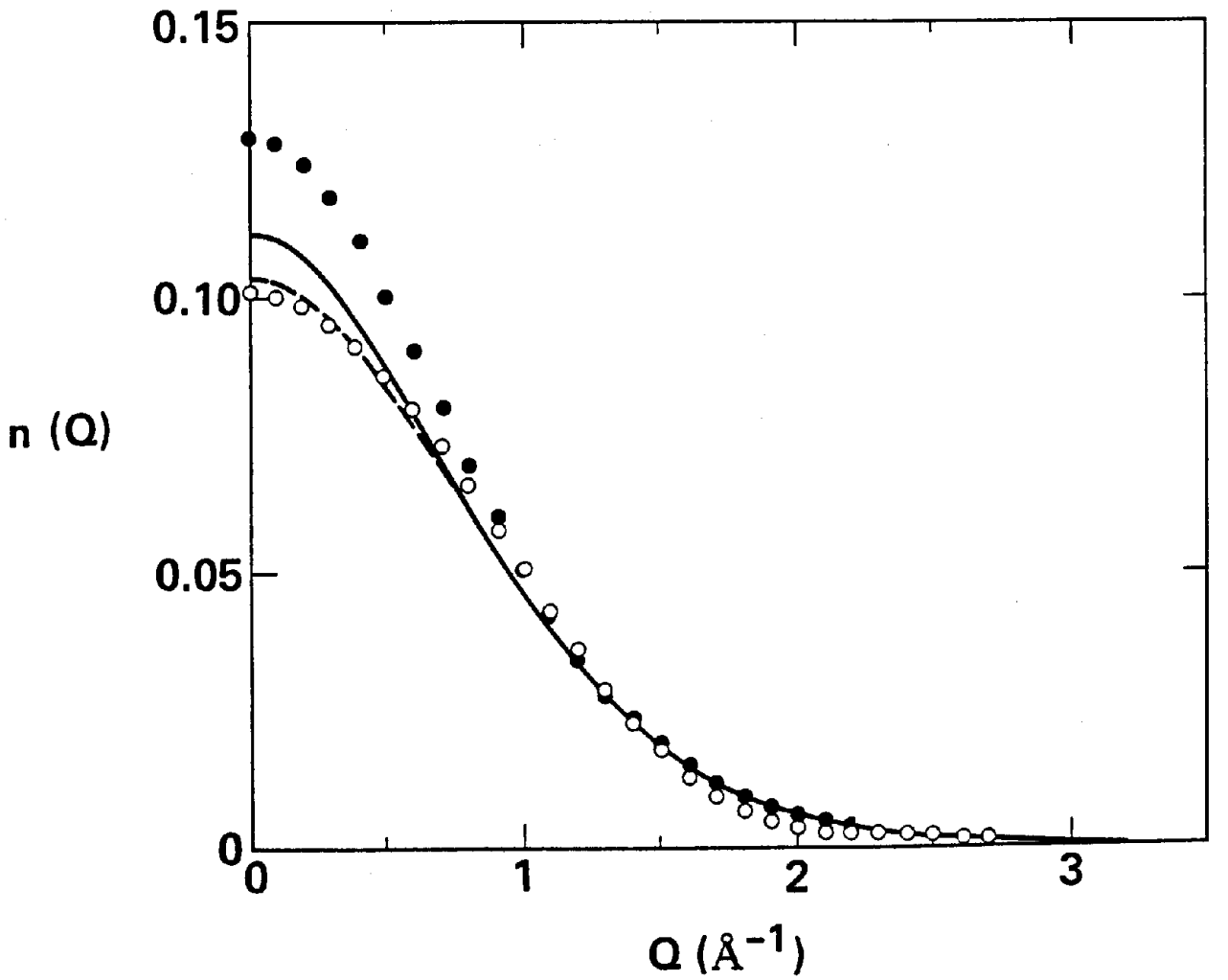

Figure 4

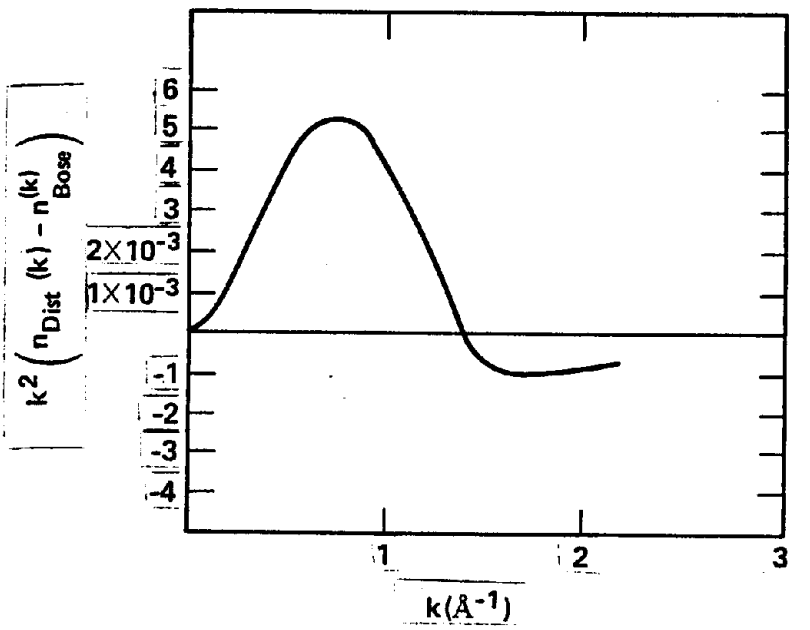
$k^2\left(n_{Dist}(k) - n^{(k)}_{Bose}\right)$
6
5
4
3
2×10^{-3}
1×10^{-3}
-1
-2
-3
-4
1
2
3
k(Å^{-1})

Figure 5

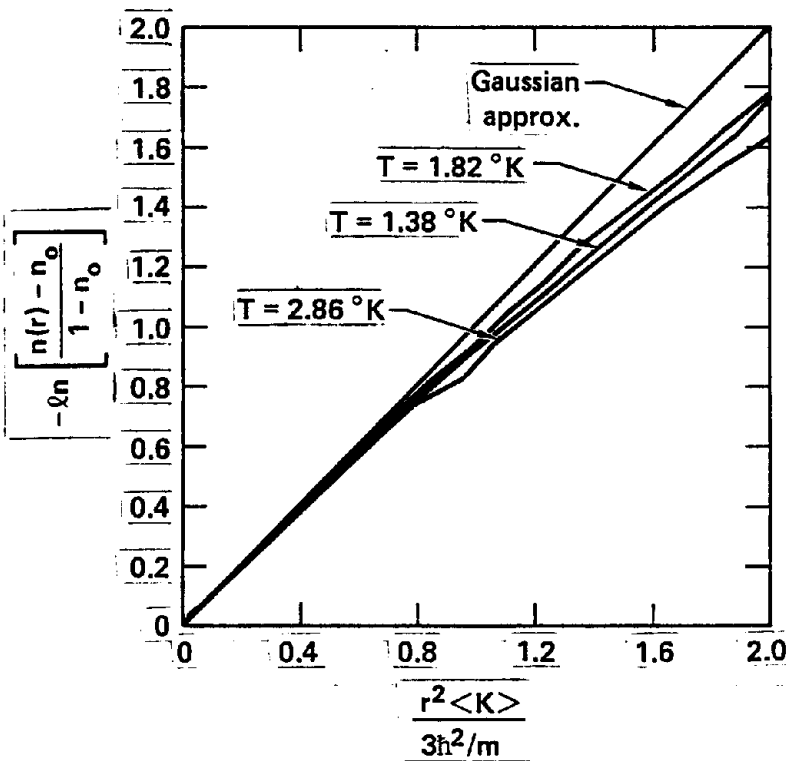
2.0
1.8
1.6
1.4
1.2
1.0
0.8
0.6
0.4
0.2
0
0
0.4
0.8
1.2
1.6
2.0
Gaussian approx.
T = 1.82 °K
T = 1.38 °K
T = 2.86 °K
$-\ln\left[\frac{n(r)-n_o}{1-n_o}\right]$
$\frac{r^2\langle K\rangle}{3\hbar^2/m}$

Figure 6

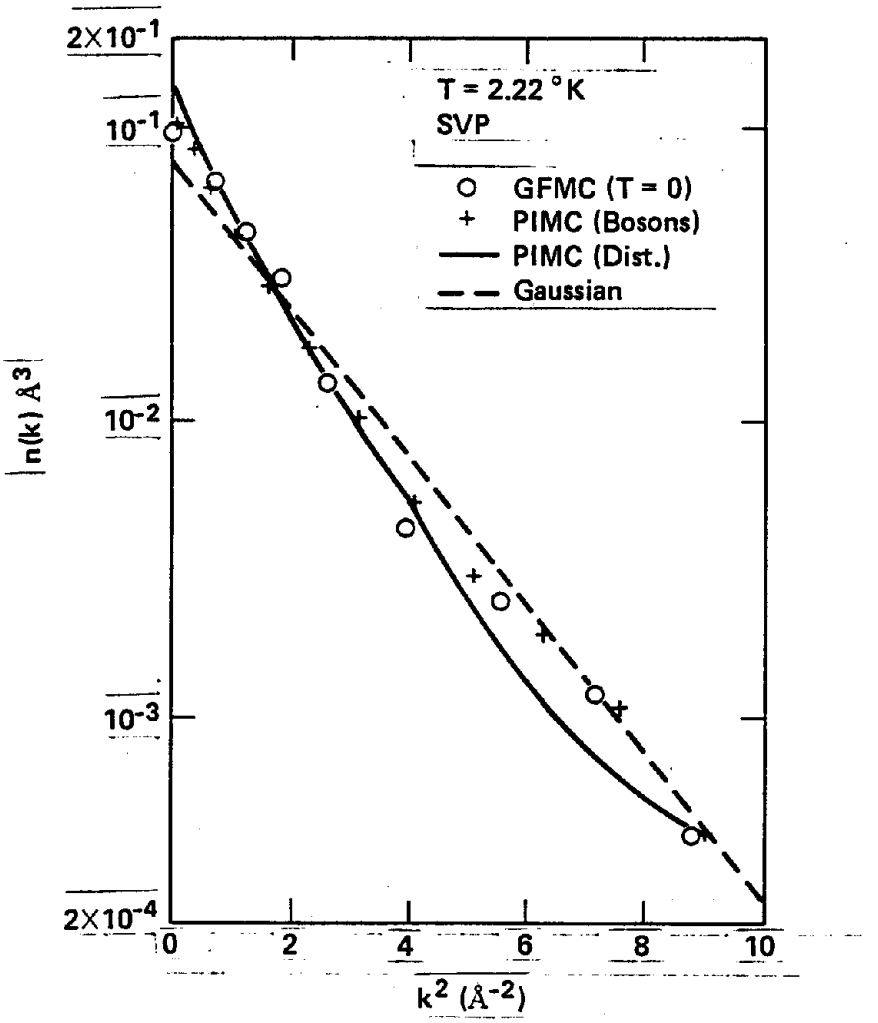
2X10⁻¹
10⁻¹
10⁻²
10⁻³
2X10⁻⁴
|n(k) Å³|
T = 2.22 °K
SVP
GFMC (T = 0)
PIMC (Bosons)
PIMC (Dist.)
Gaussian
0
2
4
6
8
10
k² (Å⁻²)

Figure 7